JOURNAL OF CATALYSIS 48, 345–353 (1977)

Improving the Poison Resistance of Supported Catalysts

L. LOUIS HEGEDUS AND JACK C. SUMMERS

General Motors Research Laboratories, Warren, Michigan 48090

Received January 24, 1977

This paper discusses the poison resistance of supported catalysts, in which the poison reacts both with the active component and the catalyst support. For such catalysts, the net rate of the poisoning reaction can be selectively manipulated with respect to the net rate of the main reaction in such a manner that a catalyst with improved poison resistance is obtained. The above statements are illustrated by diffusion-limited lead and phosphorus poisoning experiments using alumina-supported noble metal catalysts. By modifying the pore structure, support surface area, and noble metal impregnation depth of these catalysts, improvements in activity and poison resistance have been attained for automobile exhaust emission-control applications.

INTRODUCTION AND SOME THEORETICAL CONSIDERATIONS

An interesting case of impurity poisoning was discussed recently (*1*), in which not only the active component of a supported catalyst but also the support's surface itself reacts with the poison precursor. One typical example is the lead or phosphorus poisoning of alumina-supported noble metal catalysts used for automobile exhaust oxidation.

The penetration of phosphorus into a porous automobile exhaust catalyst can, at least in steady-state operation, be well described by a pore diffusion-limited poisoning mechanism (*2*). As Fig. 1 illustrates, the phosphorus penetrates the porous catalyst pellets in the form of a diffusion-limited sharp front. The same picture holds for lead poisoning in steady-state experiments [however, wide temperature fluctuatious during converter operation can cause the lead band to disperse (*3*)].

Although the automotive catalytic converter operates as an integral reactor as far as the conversion of the main reactants is concerned, this does not always hold for the poisoning reactions. High-speed photographic experiments (*4*) revealed that, under the stirring effects of the high-velocity exhaust gas, the catalyst pellets migrate continually so that, on the average, each of the individual catalyst pellets poisons at the same rate. Thus, as far as the poisoning process is concerned, it is sufficient to restrict our attention to a single catalyst pellet.

For a poisoning process which is limited by the rate of poison-precursor diffusion across the poisoned shell of the catalyst, the location of the poisoned shell (η) at time t is expressed by [e.g., Ref. (*5, 6*)]

$$t = \alpha(\tfrac{1}{2} + \eta^3 - \tfrac{3}{2}\eta^2), \qquad (1)$$

where

$$\eta = r/R, \qquad (2)$$

and

$$\alpha = c_{\mathrm{w,s}}R^2/3D_{\mathrm{p,eff}}\, c_{\mathrm{p,0}}. \qquad (3)$$

If the poison penetration depth

$$\xi = 1 - \eta \qquad (4)$$

is used, Eq. (1) converts to

$$t = \alpha(-\xi^3 + \tfrac{3}{2}\xi^2), \qquad (5)$$

ISSN 0021-9517

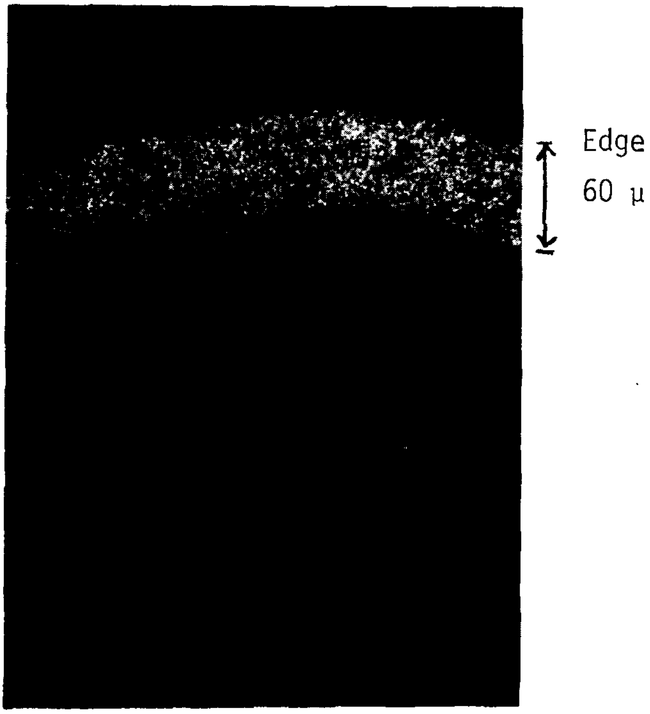

FIG. 1. Cross section of a phosphorus-poisoned spherical catalyst pellet (electron microprobe photograph).

which now expresses the time required for the diffusion-limited poisoned front to reach a dimensionless depth ξ of the catalyst pellet.

Inspecting Eqs. (1) through (5) we note that the rate of poison penetration is enhanced by more poison in the exhaust gas ($c_{\mathrm{p},0}$) or by a higher effective diffusivity ($D_{\mathrm{p,eff}}$), while it is decreased by a higher poison saturation concentration in the poisoned band (i.e., higher support surface area). Thus, as we will see, both the support surface area and the diffusivity of the poison precursor in the support's pores will be important parameters in designing improved catalysts when diffusion influences the system.

Under typical warmed-up conditions, the main reactions (oxidation of hydrocarbons and carbon monoxide) in an automotive catalytic converter are largely diffusion limited. To minimize the diffusion path of the reactants in the pores of the support, one can convincingly argue (7) for impregnating only an outer shell of the catalyst pellets which, in our case, also appears to be a prudent way to use the expensive noble-metal catalytic components. [In an interesting paper (8), it is shown that the light-off characteristics of negative-order reactions, such as the oxidation of CO over noble metals, might be improved by subsurface impregnation of the catalyst pellets.]

In the context of a finite impregnation depth ξ^* (Fig. 2), Eq. (5) can be interpreted as an expression for the time t^* at which the poison front penetrates to the depth of the impregnated shell. At this point in time, if the poisoned and impregnated zones are perfectly sharp and if the poisoned zone is inactive, the catalyst pellet will suddenly lose its activity.

It is easily seen that a practical catalyst, operating in the diffusion-limited region for both the main and the poisoning reactions, has to satisfy two simultaneous criteria. On one hand, the lifetime t^* (i.e., the time at which the poison front reaches the depth of the impregnated shell) must be longer than some specified minimum lifetime. To accomplish this safely, a deep impregnation depth is indicated. On the other hand, the catalyst also has to meet some minimum activity requirements. That is, just before the lifetime t^* is reached, the catalyst has to retain a certain fraction ϵ^* of its original activity. If the impregnation depth (and the corresponding poison penetration depth at t^*) is too large, the catalyst may lose too much of its activity before the poison reaches the impregnated depth.

For a diffusion-limited main reaction, the effectiveness factor of a partially poisoned catalyst is expressed [e.g., Ref. (9)] by

$$\beta(t) = 3 \bigg/ h^2{}_{\mathrm{a}}\left(\frac{1}{\mathrm{Bi}_{\mathrm{a}}} + \frac{\xi}{1-\xi}\right), \quad t < t^*, \qquad (6)$$

where

$$\mathrm{Bi}_{\mathrm{a}} = k_{\mathrm{a,m}}R/D_{\mathrm{a,eff}} \text{ (Biot number)}, \qquad (7)$$

and

$$h_{\mathrm{a}} = R(k_{\mathrm{a,c}}/D_{\mathrm{a,eff}})^{\frac{1}{2}} \text{ (Thiele parameter)}. \qquad (8)$$

The initial effectiveness factor (at $\xi = 0$) becomes

$$\beta(0) = 3\,\mathrm{Bi}_{\mathrm{a}}/h^2{}_{\mathrm{a}}, \qquad (9)$$

and, thus, the fraction of activity retained at time t is

$$\epsilon(t) = \frac{\beta(t)}{\beta(0)} = 1 \bigg/ \left(1 + \mathrm{Bi}_{\mathrm{a}}\frac{\xi}{1-\xi}\right), \quad t < t^*. \qquad (10)$$

For a plug-flow isothermal reactor, Eq. (10) is easily related to the conversion:

$$\epsilon(t) = \frac{-\ln[1 - X(t)]}{-\ln[1 - X(0)]}, \quad t < t^*, \qquad (11)$$

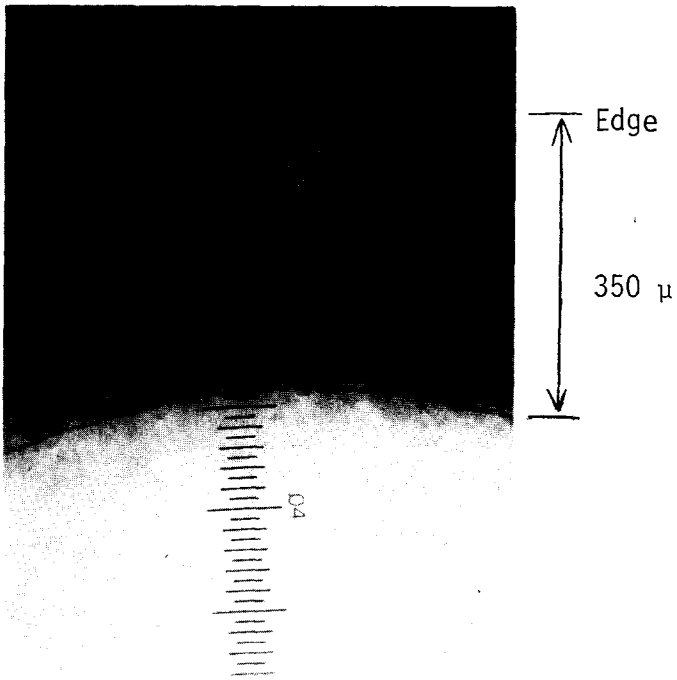

FIG. 2. Cross section of a spherical catalyst pellet showing the depth of impregnation (microscopic photography of the $SnCl_2$ developed noble metal layer).

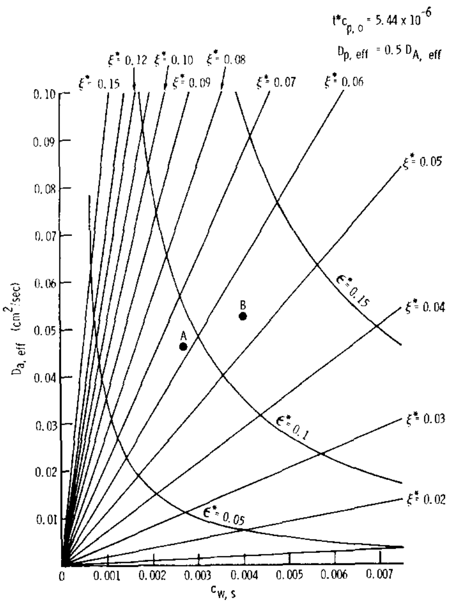

FIG. 3. Effect of catalyst design parameters on catalyst lifetime and performance. A and B are examples discussed in the text.

where $X(0)$ and $X(t)$ are the conversions at times 0 and t, respectively. The utility of Eq. (11) is readily seen: It allows one to specify $\epsilon^* = \epsilon(t^*)$, the fractional activity to be retained at a specific time t^*, as a function of the initial and final conversions required of the reactor to meet some specified standard of performance.

Equations (5) [with (3)] and (10) [with (11)] can be solved simultaneously. For a particular poison exposure $t^*c_{p,o}$ (mole seconds per cubic centimeter), Fig. 3 shows the parametric plot of $D_{a,\text{eff}}$ as a function of $c_{w,s}$ ($D_{a,\text{eff}} = 2\, D_{p,\text{eff}}$ is assumed for Fig. 3). Both the lines of constant ϵ^* and constant ξ^* are indicated, and points A and B represent examples which will be discussed later in this paper.

Figure 3 allows one to visualize the effects of changes in the design variables of diffusion-controlled catalyst pellets. In particular, it shows the effects of changes in the pore structure and surface area of the support, and shows the corresponding minimum noble metal impregnation depth ξ^* necessary to meet the particular design criteria. Since the poison exposure ($t^*\ c_{p,o}$) is a separable parameter, Fig. 3 [and Eqs. (1)–(11)] also suggest the utility of accelerated poisoning experiments by using higher poison concentrations ($c_{p,o}$) and shorter exposure times (t^*), so that their product remains equal to the number which characterizes the real-time process.

EXPERIMENTAL VERIFICATION OF MODEL ASSUMPTIONS

The diffusion-limited nature of the poison accumulation process is discussed elsewhere (*10*) in greater detail, where a good correlation was found between phosphorus accumulation experiments and a progressive shell-type model. The diffusion limited nature of the main reactions has been well established [e.g., Ref. (*11*)]. Here we discuss some further experiments to illustrate the effects of catalyst pore structure and noble metal impregnation depth.

As Eq. (5) indicated, the rate of poison penetration into the catalyst is a strong function of the effective diffusivity of the poison precursor. Since the main reactions are also diffusion limited, their rates, too, will be strongly influenced by any changes in the catalyst's pore structure. In general, a more open catalyst pore structure will facilitate the diffusion of the poison into the catalyst (thus shortening its lifetime), while it will also facilitate the diffusion

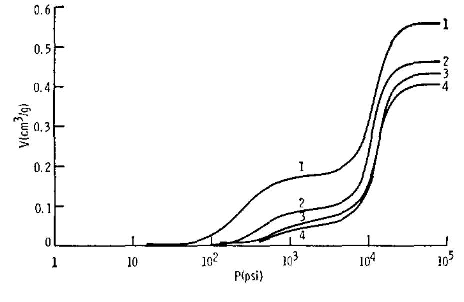

FIG. 4. Hg porosimetric curves for catalysts of varying macropore structure.

TABLE 1

Properties of Catalyst Pellets of Varying Macropore Structure[a]

	Catalyst preparation			
	1	2	3	4
ρ_p (g/cm^3)	1.150	1.293	1.358	1.441
ρ_s (g/cm^3)	3.15	3.20	3.21	3.40
V_{macro} (cm^3/g)	0.180	0.092	0.070	0.053
V_{micro} (cm^3/g)	0.372	0.369	0.355	0.347
r_{macro} (Å)	3500	2053	1562	1250
r_{micro} (Å)	67	76	67	70
s (m^2/g)	83	82	83	77
Pt (wt%)	0.1	0.1	0.1	0.1
Pb (wt%)	1.69	1.68	—[b]	1.20
P (wt%)	0.10	0.10	0.09	0.08

[a] The pellets have a disk shape, 0.495-cm diameter and 0.140-cm thickness.
[b] Not available.

of the main reactants (thus increasing the catalyst's activity at any given depth of poison penetration). This relationship was investigated in a set of simple experiments which are described below.

Four porous alumina catalysts were prepared by pressing at various pelletizer pressures, so that the macropore structure was monotonically varied, leaving the surface area and micropore structure unchanged (Fig. 4, Table 1). The resulting catalyst pellet density ρ_p varied from 1.150 to 1.441 g/cm^3, as determined by ultrahigh pressure mercury porosimetry. All the catalysts were impregnated uniformly along their radius using a hexachloroplatinic acid solution. The uniform impregnation depth was designed to eliminate impregnation depth effects in these experiments.

The four catalysts of varying macropore structure (i.e., of varying effective diffusivity) were then exposed to the poison-containing (Pb + P) exhaust of a dynamometer-mounted 5.7-liter V-8 engine. The fuel contained 0.10 g/liter of Pb and 0.005g/liter of P, and the exposure time was 35 hr for all four catalysts. At the end of the 35-hr steady-state exposure, the activity of the catalysts was tested in a laboratory reactor using simulated exhaust at 85,000 hr^{-1} (STP) space velocity, at 550°C reactor inlet temperature.

Electron microprobe experiments showed that indeed, as before, the poisons penetrated the catalyst pellets in the form of sharp progressive shells. Figure 5 shows that the activity of the poisoned catalysts is

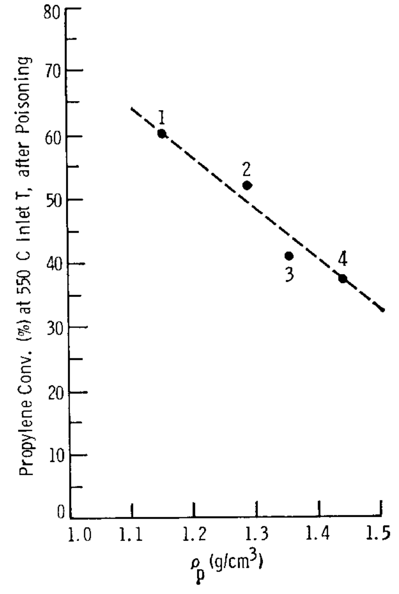

FIG. 5. Propylene conversion (at 85,000-hr^{-1} space velocity) after 35 hr of poisoning in an accelerated test, for catalysts of varying macropore volume.

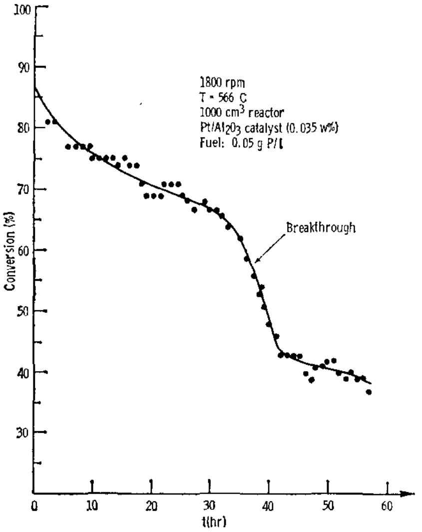

Fig. 6. Hydrocarbon conversion as a function of time in an accelerated phosphorus poisoning experiment.

higher if the density is lower (i.e., if the diffusivity is larger). This indicates that an increase in macropore size, at least in the range of operating and catalyst design parameters of this experiment, results in a net improvement in catalyst performance, despite the fact that the lower density catalysts picked up somewhat more poison (Table 1). Note that the experiment described here corresponds to moving along a constant $c_{w,s}$ line toward higher diffusivities in Fig. 3, which correctly predicts higher performance (higher ϵ^*) at a constant exposure.

The importance of catalyst impregnation depth is demonstrated by another experiment. In this, porous alumina pellets were impregnated to a depth of about 42 μm below their surface. An aqueous chloroplatinic acid solution was used, and the catalyst contained 0.035 wt% Pt. About 1000 cm³ of these pellets was placed into an experimental reactor which was designed to allow catalyst sample withdrawal at four different bed depths, after various poison-exposure times. The reactor is described in Ref. (10). It is essentially isothermal, and the space velocity is so high [about 110,000 hr^{-1} (STP)] that the poison concentration profiles along the bed depth are reasonably flat.

The above experimental reactor was connected to the exhaust of a 5.7-liter V-8 engine which was mounted on an engine dynamometer. The engine was run on a phosphorus-containing fuel (0.05 g of P/liter). As we monitored the hydrocarbon concentration against time (Fig. 6), a sudden drop in activity occurred beyond about 30 hr of exposure time. Electron microprobe analysis of the poisoned catalyst samples (Fig. 7) revealed that, indeed, the poison front reached the noble metal impregnation depth at the time the activity drop was observed. This provides a welcome qualitative verification of the simple model discussed in the previous part of this paper. Due to the high space velocity and the corresponding flat poison profiles along the reactor's length, the activity drop is reasonably sharp here, indicating that the poison reaches the impregnated depth approximately at the same time for most of the catalyst pellets in the reactor. For lower space velocities and corresponding steeper poison profiles along the reactor's length, the activity drop would, of course, be less sudden.

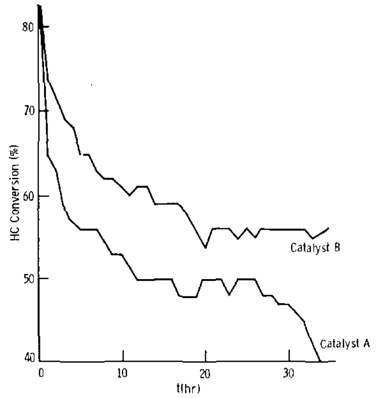

Fig. 8. Comparison of the performance of two catalysts (see Table 2) in an accelerated durability test at high space velocity. Catalyst B is a redesigned counterpart of catalyst A.

It is noteworthy to observe that the activity of the poisoned catalyst in this experiment did not drop to zero after the poison exceeded the noble metal impregnation depth. Such a "residual" activity has often been observed by us with automotive catalysts (*2*). A theoretical discussion of poisons with finite activity is provided in a recent note (*12*).

DESIGN OF AN IMPROVED CATALYST FOR AUTOMOBILE EXHAUST OXIDATION

In order to improve the conversion performance of the catalyst, we have to increase the effective diffusivity of the reactants across the poisoned shell. However, larger catalyst pores would also increase the rate of poison penetration [Eq. (5)]. The important observation here is that, according to Eq. (5), the diffusion-limited rate of poison penetration into the pellet can be kept under control by increasing the surface area of the support. This will increase the saturation concentration of the poison in the catalyst, making use of the fact that the support reacts with the poison precursors and acts as an effective "trap" for them.

In principle, it might be possible to think of some optimum catalyst configuration. However, practical considerations (maximum stable surface areas at the reactor operating temperature, physical and mechanical constraints and resulting materials limitations, complexity of operating conditions and feedstream, etc.) suggest that an improvement in catalyst performance is a more realistic goal than to seek an absolute optimum, even if the assumption is made that such an optimum exists.

Table 2 compares the parameters which characterize a catalyst (A) and its redesigned counterpart (B) for automotive applications. Catalyst B has larger macropores to facilitate the diffusion of reactants across the poisoned zone, larger surface area to reduce the rate of poison progression, and a somewhat deeper noble metal impregnation depth to ensure an adequate lifetime. The small differences in their noble metal contents were found to be unimportant in these almost completely diffusion-limited high-temperature experiments.

TABLE 2

Example for Improving a Catalyst: Catalyst B Has Improved Performance Over Catalyst A

	A	B
s (m^2/g)	94	135
ρ_p (g/cm^3)	1.132	1.052
$\bar{r}_{macro}$ (Å)	6270	10872
$\bar{r}_{micro}$ (Å)	90	73
V_{macro} (cm^3/g)	0.140	0.170
V_{micro} (cm^3/g)	0.461	0.497
ρ_{solid} (g/cm^3)	3.54	3.53
Impregnation depth (μm ± 1 SD)	39±9	103±20
Pt (wt%)	0.0350	0.0430
Pd (wt%)	0.0137	0.0190
Dispersion by H_2 titration (%)	40	60
Area of metal/volume of pellet (cm^2/cm^3)	702	1262
Area of metal/weight of pellet (cm^2/g)	620	1200
HC conversion (%)[a]		
0 hr	79	83
35 hr	40	56

[a] Accelerated poisoning test in a 1000-cm^3 reactor at a space velocity of about 110,000 hr^{-1} (STP). $T = 566$°C; fuel composition: 0.10 g/liter of Pb, 0.005 g/liter of P.

The design parameters of catalyst A and the path leading to catalyst B are shown in Fig. 3. Catalyst A is impregnated to a depth of 2.5% of its radius. Figure 3 suggests that a deeper noble-metal impregnation depth (8.5% of the radius) would be necessary to avoid premature poison breakthrough across the active layer.

Catalyst B has a redesigned support: Its higher surface area resulted in a higher value of $c_{w,s}$ (*2*), and its larger macropores

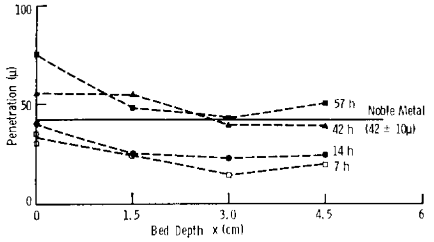

FIG. 7. Phosphorus penetration depths as a function of time and location in the reactor bed, for the experiment shown in Fig. 6. (Electron microprobe measurements on individual catalyst pellets.)

resulted in a lower density and a higher effective diffusivity [as calculated from the random pore diffusivity model (*13*)]. The net result is that a higher conversion performance is indicated after a specified poison exposure, as shown in Fig. 3. Comparison of the design parameters of catalyst A and B with Fig. 3. suggests that support B should be superior to support A at their corresponding optimal impregnation depths, and that the actual impregnation depth of A is too shallow to meet the design life of the catalyst. Indeed, when exposed to a lead and phosphorus containing exhaust of an automobile engine [1000-cm^3 reactor, 5.7-liter V-8 engine, space velocity ~110,000 hr^{-1} (STP), increased Pb and P levels in the fuel to simulate 80,000 km in about 40 hr], catalyst B showed a significantly improved poison resistance (Fig. 8). The rapidly declining activity of catalyst A beyond the 30-hr mark was shown (by electron microprobe) to be due to the fact that the poisons reached the noble-metal impregnation depth, similar to the example of Figs. 6 and 7.

The discussions in this paper regarding the activity of partially poisoned automotive catalysts are of necessity only semiquantitative. Despite this, the strategy outlined here provided the authors with directions for meaningful experimentation which resulted in improved steady-state catalyst performance after a minimum number of experiments.

NOMENCLATURE

$c_{\mathrm{p,0}}$ (mole/cm^3 of gas)	Poison precursor concentration in exhaust gas
$c_{\mathrm{w,s}}$ (mole/cm^3 of pellet)	Saturation poison concentration in catalyst pellet
Bi_{a}	Biot number (see text)
$D_{\mathrm{a,eff}}$ (cm^2/sec)	Effective diffusivity of main reactant
$D_{\mathrm{p,eff}}$ (cm^2/sec)	Effective diffusivity of poison precursor
h_{a}	Thiele parameter (see text)
$k_{\mathrm{a,m}}$ (cm/sec)	Mass transfer coefficient
$k_{\mathrm{a,c}}$ (cm/sec)	First-order rate constant
r (cm)	Pellet radial coordinate
r (Å)	Pore radius (frequency peak, Table 1 and Fig. 4)
$\bar{r}$ (Å)	Integral averaged pore radius (Table 2)
R (cm)	Radius of catalyst pellet
t (sec)	Time
t^* (sec)	Lifetime of catalyst (see text)
x (cm)	Reactor axial coordinate
X	Fractional conversion in an integral, plug-flow reactor
V (cm^3/g)	Catalyst pore volume
α (sec)	Constant (see text)
β	Effectiveness factor (see text)
ϵ^*	Fraction of initial activity retained just before t reaches t^*
ξ	Dimensionless penetration depth $= 1 - r/R$
ξ^*	ξ at t^*
$\eta = 1 - \xi = r/R$	Dimensionless pellet radial coordinate
ρ_{p} (g/cm^3)	Pellet density
a (subscript)	Reactant
p (subscript)	Poison precursor
w (subscript)	Poison

ACKNOWLEDGMENTS

Thanks are due to R. Richmond (engine dynamometer experiments), A. Ottolini and T. Schreiber (electron microprobe), C. Schaefer (pellet pressing experiments), P. Mitchell (laboratory oxidation reactor experiments), and S. H. Oh (for computing Fig. 3).

REFERENCES

1. Hegedus, L. L., *Ind. Eng. Chem. Fundam.* **13**, 190 (1974).
2. Hegedus, L. L., and Summers, J. C., Paper presented at the Fourth North American Meeting of The Catalysis Society, Toronto, Ontario, Canada, February 18, 1975. General Motors Research Publication No. GMR-1823, February 1975.
3. Klimisch, R. L., Summers, J. C., and Schlatter, J. C., *Advan. Chem. Ser.* **143**, 103 (1975).
4. Komarmy, J. M., Personal communications. AC Spark Plug Division, General Motors Corporation, Flint, Mich., 1974.
5. Carberry, J. J., and Gorring, R. L., *J. Catal.* **5**, 529 (1966).
6. Levenspiel, O., "Chemical Reaction Engineering," 2nd ed. John Wiley, New York, 1972.
7. Minhas, S., and Carberry, J. J., *J. Catal.* **14**, 270 (1969).
8. Wei, J., and Becker, E., *Advan. Chem. Ser.* **143**, 116 (1975).
9. Bischoff, K. B., *Ind. Eng. Chem. Fundam.* **8**, 665 (1969).
10. Hegedus, L. L., and Baron, K., Paper presented at the joint VDI-GVC and AIChE meeting, Munich, W. Germany, September 1974. General Motors Research Publication No. GMR-1615, August 1974.
11. Hegedus, L. L., and Cavendish, J. C., *Ind. Eng. Chem. Fundam.*, in press, 1977.
12. Hegedus, L. L., *Chem. Eng. Sci.* **29**, 2003 (1974).
13. Smith, J. M., "Chemical Engineering Kinetics," 2nd ed. McGraw-Hill, New York, 1970.